World Academy of Science, Engineering and Technology
International Journal of Electrical and Computer Engineering
Vol:9, No:11, 2015

Evaluation of Methodologies for Measuring Harmonics and Inter-Harmonics in Photovoltaic Facilities

Anésio de Leles F. Filho, Wesley R. de Oliveira, Jéssica S. G. Pena, Jorge A. C. Angarita

Open Science Index, Electrical and Computer Engineering Vol:9, No:11, 2015 publications.waset.org/10003180.pdf

***Abstract*—**The increase in electric power demand in face of environmental issues has intensified the participation of renewable energy sources such as photovoltaics, in the energy matrix of various countries. Due to their operational characteristics, they can generate time-varying harmonic and inter-harmonic distortions. For this reason, the application of methods of measurement based on traditional Fourier analysis, as proposed by IEC 61000-4-7, can provide inaccurate results. Considering the aspects mentioned herein, came the idea of the development of this work which aims to present the results of a comparative evaluation between a methodology arising from the combination of the Prony method with the Kalman filter and another method based on the IEC 61000-4-30 and IEC 61000-4-7 standards. Employed in this study were synthetic signals and data acquired through measurements in a 50kWp photovoltaic installation.

***Keywords*—**Harmonics, inter-harmonics, IEC61000-4-7, parametric estimators, photovoltaic generation.

I. Introduction

THE increasing demand for energy resources with low environmental impact has increased the participation of alternative energy sources in the global matrix. Among them, photovoltaic stands out, which has received governmental and private agent incentives and consequently has presented to be more attractive and competitive daily. However, in recent decades, it has been necessary to investigate the impact caused by grid connected operation of alternative sources. This occurs mainly because in these systems, devices that cause harmonics and inter-harmonics such as electronic converters are employed [1]. Frequently, in a low power quality, these equipments have a low embodied cost [2].

A challenge in the study involving harmonics and inter-harmonics in electric power network is concentrated on the choice of methodology that could allow the proper identification of the levels of distortion in electric currents and voltages.

The signal analysis methods traditionally used in recommendations/standards that deal with this subject are based on the use of Discrete Fourier Transform (DFT), as sampled by IEC 61000-4-7. This standard is used to estimate the spectrum and calculate the distortion indexes and has been one of the main references in this line of work. Meanwhile, IEC 61000-4-30 is responsible for proposing measurements protocols that should be employed. It should be emphasized that, according to the aspects demanded for the implementation of DFT, i) the signals in question must be periodic, ii) the sampling of the signals must meet the Nyquist criterion and iii) each frequency contained in the signal must be a multiple integer of the fundamental frequency previously assumed in the algorithm [3]. Having said that, it is understood that two aspects can make the results from the Fourier analysis inaccurate, namely i) the variation in time of the harmonic and inter-harmonic components amplitudes [3], and ii) the variation in time of the fundamental signal component period [4]. In fact, these two aspects can culminate in the emergence of spurious components in the spectrum, which is not consistent with the true signal components. In this context, the application of parametric technics in the identification of frequencies is an alternative which has been used in literature [5], [6]. Among the advantages linked to the parametric method application, the possibility of conducting a windowing for a non-integer number period of signals can be emphasized. Besides that, they can be associated with amplitude tracking methods like Kalman filter. An example of parametric technics is the frequency estimator known as the Modified Prony Method, which can be combined with a Bayesian linear method, implemented by means of a Kalman filter [4]. In this methodology, the amplitudes of the sinusoids present in the analyzed signals are estimated by the Kalman filter and the filter regressors are built through the frequencies provided by the Modified Prony Method [4]. This method can be adapted to monitor signals from photovoltaic installations.

Considering the questions mentioned herein, this work seeks to present the results of a comparative evaluation between a measurement method based on the IEC 61000-4-30 and IEC 61000-4-7 standards and another from the combination of the Prony Method with Kalman Filter. Therefore presented firstly are the two methods of measuring distortion in an electric power system. Thereafter, the procedure used in this study to comparatively evaluate the results obtained in each one, in a synthetic signal analysis and a real signal acquired in a 50kWp photovoltaic installation is detailed. Finally, the results and conclusions are presented in order to make possible not only the comparison of methods, but also, the verification of the behavior in time and frequency of the signals used.

A. L. Ferreira Filho and J. A. C. Angarita are with the University of Brasilia, Brasilia, Brazil (e-mail: leles@unb.br, jcormane@unb.br).

Open Science Index, Electrical and Computer Engineering Vol:9, No:11, 2015 publications.waset.org/10003180.pdf

II. Measurement Methodologies of Distortions in Electric Power System

A. IEC 61000-4-30/61000-4-7Methods

The analysis of the levels of distortion of the waveforms starts by obtaining the spectrum. In standards IEC 61000-4-7 [7] and IEC 61000-4-30 [8], the spectral decomposition is carried out through DFT.

The scope of the IEC 61000-4-7standard comprises of the instrumentation and measurement of spectral components that are superimposed on the 50 Hz or 60 Hz fundamental electric power systems. A key aspect in this standard is the grouping of the spectral bars. Fig. 1 shows the groups and subgroups formed by employing the IEC 61000-4-7 standard.

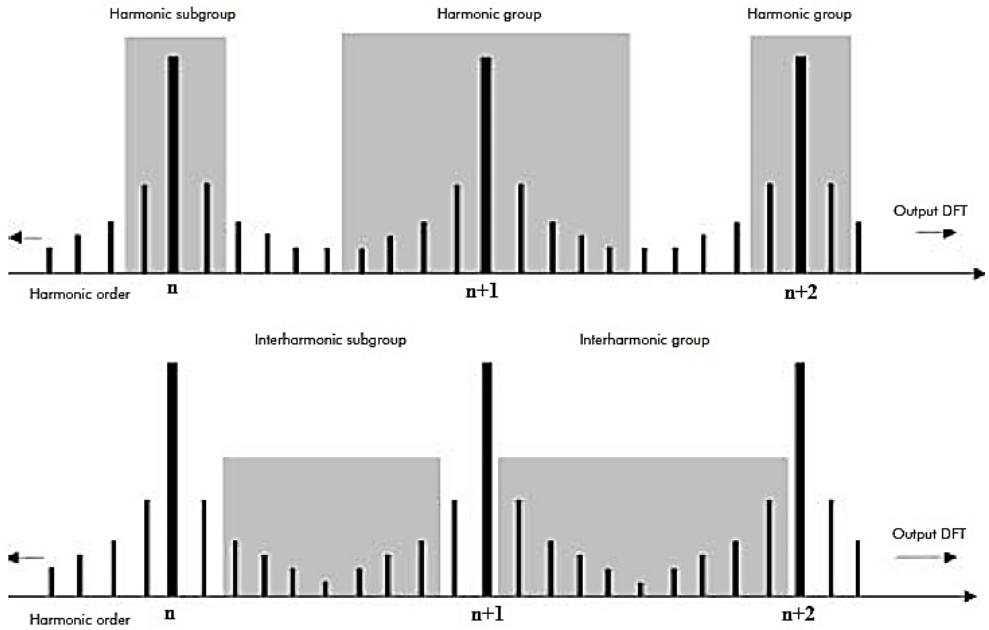

Fig. 1 Groups and subgroups from the IEC 61000-4-7 standard [9]

In Fig. 1, the concept that defines the RMS amplitudes of various groups and subgroups can be observed. The subgroup of the *nth* harmonic, for example, has its RMS value given by the aggregation of the two spectral bars immediately adjacent the harmonic crossbar. An inter-harmonic subgroup includes all the bars between two consecutive harmonics, with exception to those which are adjacent to these.

The results from IEC 61000-4-7 can be aggregated in time, as shown in IEC 61000-4-30. The IEC 61000-4-7 specifies the measurement equipment in three classes of performance: A, S and B. For class A, dealt in the scope of this work, the magnitude measurement interval of various parameters of the electric energy quality should be 12 cycles for 60 Hz power systems, that is 200ms [8]. These parameters are then aggregated at regular time intervals, as shown in Fig. 2.

The joint application of this method consists in:

a. The processing of the signals every 200ms by DFT. It should be noted, among other technical considerations that the signals must be obtained with a PLL synchronization (*phase locked loop*), and the minimum recommended sampling rate must be 128 samples per 60 Hz cycles;
b. Perform grouping and smoothing of the results;
c. Calculate the individual and global distortion indexes like THD (Total Harmonic Distortion). Also employed in this study, is the TID (Total Inter-harmonic distortion), as defined in (1);

$$TID = \sqrt{\sum_{u=0.5}^{U}\left(\frac{G_{isg,u}}{V_1}\right)^2} \quad (1)$$

where: U is the highest group of interharmonics, $G_{isg,u}$ is the *u-th* evaluated inter-harmonic subgroup amplitude, and V_1 is the fundamental component.

d. Aggregation 1: The aggregation process at intervals of 180 cycles, in a way that it forms 15 subdivisions of 12 cycles. Repeat steps (a)-(c) and aggregate the results for each 3s;
e. Aggregation 2: The aggregation process at intervals of 3.600 cycles, in a way that it forms 300 subdivisions of 12 cycles. Repeat steps (a)-(d) and aggregate the results for each 1 min;
f. Aggregation 3: The aggregation process at intervals of 36.000 cycles, in a way that it forms 3.000 subdivisions of 12 cycles. Repeat steps (a)-(e) and aggregate the results for each 10min.

B. Prony/Kalman Method (PK)

The proposed methods in [4], combines the parametric estimator of Prony and Kalman Filtering. Prony estimator provides the frequencies, while Kalman estimator provides the

temporal evolution of the amplitudes of the sinusoidal components present in the analyzed signal.

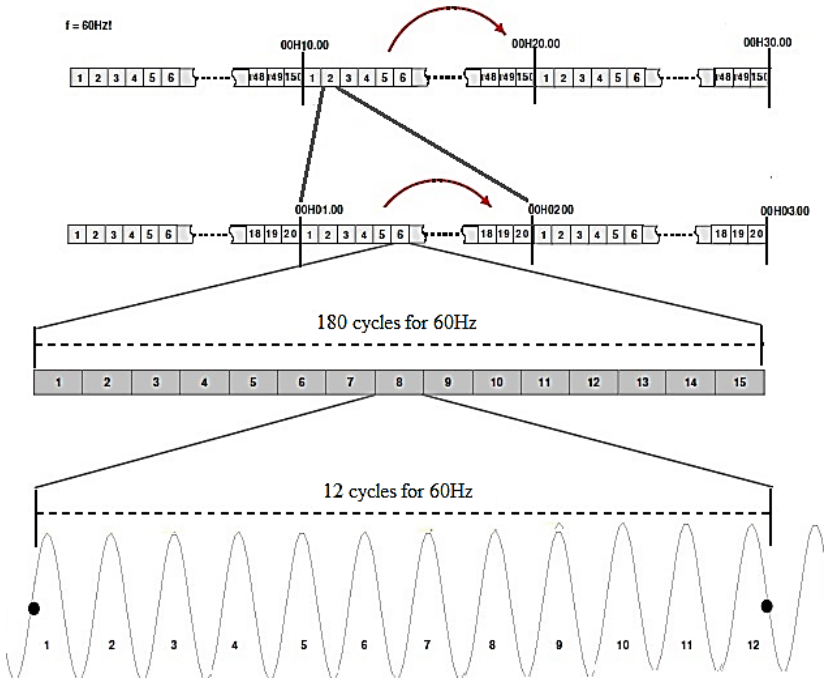

Fig. 2 Aggregation at nominal frequency (60Hz)

In this approach, the author proposes an adaptation of the Prony classic method [10], calling the new algorithm Modified Prony (MP). In order to develop this method, it was assumed that the signal $y[n]$ consists of p sinusoidal components, and was also considered that the frequency parameters returned by the Prony Classic method are in fact poles of successive digital filters with coefficients b_k applied to the signal as shown in (2):

$$\begin{aligned} &y_1[n] = y[n], \rightarrow n = 1,2,..., N, \\ &y_2[n]=y_1[n-1]+b_1 y_1[n]+y_1[n+1], \rightarrow n=2,...,(N-1), \\ &y_3[n]=y_2[n-1]+b_2 y_2[n]+y_2[n+1], \rightarrow n=3,...,(N-2), \\ &\vdots \\ &y_{p+1}[n] = y_p[n-1] + b_p y_p[n] + y_p[n+1], \rightarrow n = p+1,..., (N-p+1), \end{aligned} \tag{2}$$

The b_k coefficients are obtained through (3):

$$b_k = -2\cos(\omega_k T_s) \tag{3}$$

where: ω_k is the frequency and T_s is the sampling rate.

If the frequencies contained in the signal were correctly estimated, then coefficients b_k also will, and the filtering process shown in (2) results in a residual vector $\boldsymbol{y_{p+1}}$, whose norm iszero. The method proposed in [4] uses this fact to present a deterministic optimization procedure which aims to find the b_k coefficients that minimizes this norm.

An advantage of this approach is the possibility of incorporating an FIR (Finite Impulse Response) filtering procedure, which helps to attenuate the degenerative noise effect in the data signal. The procedure for determining this digital filter $\boldsymbol{w}$ is iterative and consists in successively applying the MP method and solving the least squares problem shown in (4):

$$\begin{aligned} &a * w = \delta[n] + e[n] \\ &\min \upsilon[n] = \sum_{n=1}^{p+q} e^2[n] \end{aligned} \tag{4}$$

where Prony vector $\boldsymbol{a}$ has a size of $p+1$. It is determined according to (5), wherein (*) represents the convolution operation. The digital filter $\boldsymbol{w}$ is assumed to have a size q, and $e[n]$ represents the error in relation to the unit vector impulse $\delta[n]$, expected as the result of the convolution in (4).

$$a = \begin{bmatrix} 1 & b_p & 1 \end{bmatrix} * \begin{bmatrix} 1 & b_{p-1} & 1 \end{bmatrix} * \cdots * \begin{bmatrix} 1 & b_2 & 1 \end{bmatrix} * \begin{bmatrix} 1 & b_1 & 1 \end{bmatrix} \tag{5}$$

The Kalman Filter (KF) belongs to the linear Bayesian estimator class. The Bayesian estimation assumes that there are available statistical models for both $y[n]$ signal, which is considered a stochastic process, and for the parameters to be estimated [11]. For the application of this estimation method, it is considered that each sinusoidal component $C_i[n]$ in the signal is written as (6) [4]:

$$\begin{aligned} C_i[n] &= A_i \cos(\omega_i T_S n + \theta_i) \\ &= A_i \cos(\theta_i)\cos(\omega_i T_S n) - A_i sen(\theta_i) sen(\omega_i T_S n) \end{aligned} \tag{6}$$

Open Science Index, Electrical and Computer Engineering Vol:9, No:11, 2015 publications.waset.org/10003180.pdf

where A_i is the amplitude of the *i-th* component; ω_i is the frequency estimated by Prony T_s is the sampling; θ_i is the phase component.

The state space model used for this case is (7):

$$\begin{aligned} x_{n+1} &= \Phi_n x_n + \omega_n \\ y[n] &= h_n x_n + \eta[n] \end{aligned} \tag{7}$$

where $\boldsymbol{x}_n$ is a vector (*2px1*) that represents the amplitudes of the sinusoidal components in time according to (8); $\boldsymbol{\phi}_n$ is an identity matrix (*pxp*); $\boldsymbol{w}_n$ is a vector (*px1*) that represents the uncorrelated process noise in time with the covariance matrix Q; $y[n]$ is the data signal; $\boldsymbol{h}_n$ is the vector of the regressor model (*2px1*), whose elements are given in (9); and $\boldsymbol{\eta[n]}$ represents the measurement of white noise with a variance *r*.

$$\begin{aligned} x_i[n] &= A_i[n]\cos(\theta_i) \rightarrow i = 1,3,5,\cdots,2p-1 \\ x_i[n] &= A_i[n]\sin(\theta_i) \rightarrow i = 2,4,6,\cdots,2p \end{aligned} \tag{8}$$

$$\begin{aligned} h_i[n] &= \cos(\omega_i \Delta T n) \rightarrow i = 1,3,5,\cdots,2p-1 \\ h_i[n] &= -\sin(\omega_i \Delta T n) \rightarrow i = 2,4,6,\cdots,2p \end{aligned} \tag{9}$$

Based on the presented model, the Kalman filtering is applied as described in [12]. Given that the Prony frequency estimation process is non-linear, it consumes more processing time than the Kalman tracking amplitude stage. Therefore, in [4], the author tracks the amplitudes continuously, but with the frequency information estimated to more widely spaced time intervals.

In this work, the application of the methodology is performed as follows:

a. Processes the signal with the MP algorithm with 6% of the data signal files to perform the estimation of frequencies in the current window. This initial process is repeated every 10 files. Although the resolution of the Prony method is almost unlimited, this work is restricted to the use of integer frequencies;
b. Processes the current file, which contains a 1s window of the signal, with KF, using the last valid frequencies estimation;
c. Aggregation 1: the average of the obtained evolutions are calculated in (b) and then they are stored for the sub-windows of 12 cycles and for every 1s;
d. Aggregation 2: repeats steps (a) - (b) - (c) by carrying out the same aggregations to 3s, 1min and 10min intervals.

III. Methodology

In this work, the comparative evaluations of the results returned by the IEC and PK methods are developed. For this, syntheticand real signals are employed. As a general procedure, 1s time windows are obtained from the data signal, which is sampled every 30s. Each 1s window yields a file to be analyzed by each method. The real data were acquired at a sampling rate of 256 samples per 60 Hz cycle and a rate of 128 samples per cycle was adopted in the simulations.

For the synthetic signal shown in (10), the use of each method on a 30 minutes measurement is replicated.

$$\begin{aligned} y(t) &= A(t)\cdot\cos(2\pi 60t) + 30\cdot\cos(2\pi 30t) + 60\cdot\cos(2\pi 300t) \\ &+ 70\cdot\cos(2\pi 420t) + 20\cdot\cos(2\pi 435t) + 80\cdot\cos(2\pi 735t) \\ &+ 25\cdot\cos(2\pi 1140t) + 25\cdot\cos(2\pi 1250t) \end{aligned} \tag{10}$$

Where *A(t)* represents an amplitude of200 p.u. modulated by a5 Hz triangular wave oscillating between 0.8 and 1.2 p.u..

The selection of the frequencies that compose *y(t)* was based on the observation of a real current signal obtained at the output of a frequency inverter. It is noteworthy that, from (10), the values of the amplitudes and phases of the harmonics and inter-harmonics that should be identified by the methods in evaluation are absolutely known.

The values determined for each method for the P95% of the following parameters are evaluated subsequently: THD, TID, Fundamental Magnitude, Individual Harmonic Distortions of the 5th, 7th and 19th orders, and the inter-harmonic subgroups 0, 7, 12 and 20 [7]. Since the real values of these parameters are known, the differences between these values and the results yielded by each method can be computed. These errors are used to perform the comparison between the methods.

As the signal varies over time, the real spectrum also evolves over time. Thus, the methods tend to present spectra which change during the period of measurement. This means that the above parameters also evolve over time. Therefore, the maximum instantaneous errors (MEI) are computed. To calculate the MEI, the percentage difference between the values returned by the methodologies for each minimum of 12 cycles with respect to the expected values for each parameter to the end of that period is initially calculated. Once the error for each window is identified, the MEI will represent the maximum error value observed during a 30 minutes measurement period.

The real signals used correspond to the waveforms of the current from a 50kWp PV installation, located in Brasilia, connected 24 hours a day to the network. The signals were measured in the coupling point of the photovoltaic system to the distribution network, at the output of the frequency inverters. In this work, the phase A current signals were used in the analysis of a day of measurement.

The measurements were performed with Class A PQ analyzer. This equipment ensures the continuous sampling of the signals at the required rate, the conditioning of the signals and the PLL synchronization. In the case of the real signals, the comparative analyzes are performed considering the P95% values obtained for the following parameters by each method: THD, TID, RMS of the Fundamental, Individual Harmonic Distortions of 2nd, 3rd and 5th order, and the 0, 1 and 2 subgroups of inter-harmonics.

Open Science Index, Electrical and Computer Engineering Vol:9, No:11, 2015 publications.waset.org/10003180.pdf

Open Science Index, Electrical and Computer Engineering Vol:9, No:11, 2015 publications.waset.org/10003180.pdf

IV. Results and Discussions

A. Synthetic Signals

Fig. 3 shows a 200 ms view of the synthetic waveform signal obtained from (10).

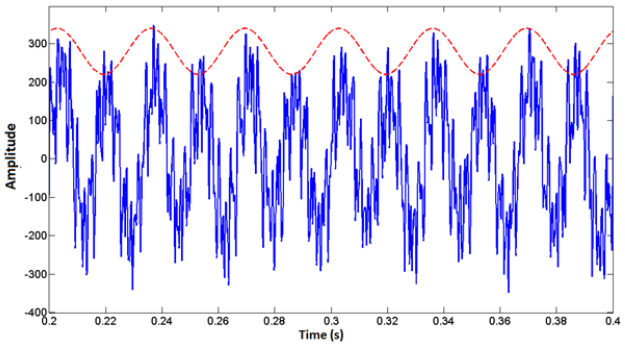

Fig. 3 Synthetic Signal Waveformy(t)

Besides the characteristic distortion caused by the harmonics and the amplitude variation of the fundamental, the waveform modulation effect (red curve) is noted in Fig. 3, which is related to the presence of inter-harmonics [9]. In this case, the temporal variation presented in the signal is reflected in the behavior of the distortion indices.

Fig. 4 shows the time variation of the THD and TID indexes. With the use of an algorithm, it is possible to identify that the theoretical P95% values for the THD and TID indexes are, respectively, equal to 59.0% and 56.3%.

Table I shows the errors resulting from the use of the IEC and PK methods, when calculating the parameters mentioned herein. The errors in percentage refer to the theoretical values of the parameters.

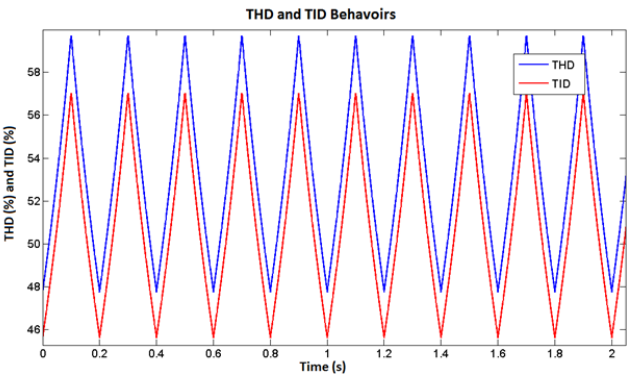

Fig. 4 Expected evolution of the THD and TID indexes in the simulation

From Table I, errors up to 10.9% and 11%, both related to the application of DFT, are verified for P95% and MEI, respectively. This occurs because the spectral estimation of a signal using the IEC assumes the signal to be periodic, that is, it repeats itself every 12 window cycles. Due to this, in the case of time-varying signals, the DFT results related to the IEC groups and subgroups do not represent the entire signal energy [4]. The errors committed in the calculation of the indices of distortion over time can be significant due to the signal variation within the Fourier window.

TABLE I
Errors in the Calculation of Parameters According to the IEC and PK Methods

Parameters	P95%		MEI	
	IEC	PK	IEC	PK
THD	10,8%	1,4%	10,9%	1,2%
TID	10,9%	2,3%	11%	2,4%
60 Hz	9,0%	0,54%	9,8%	0,87%
5ª	9,8%	0,80%	10,9%	0,90%
7ª	9,8%	0,95%	10,9%	0,95%
19ª	9,8%	1,0%	10,9%	1,1%
Sub. IH 0	9,8%	1,2%	10,9%	1,5%
Sub. IH 7	9,8%	0,60%	10,9%	0,95%
Sub. IH 12	9,8%	1,1%	10,9%	1,2%
Sub. IH 20	9,8%	0,80%	10,9%	0,90%

Also in Table I, it is noted that the PK method presented the smallest errors in the determination of the individual distortions. This occurred because the frequencies identified by Prony were not affected by the temporal variation of the signal. Additionally, Kalman filtering permitted the tracking of amplitude variations.

Fig. 5 shows the time-frequency diagram obtained by processing the signal with PK. The visualization was expanded to the first 5 seconds of simulated time. The colors variations represent, according to the graduated scale on the right, the evolution of the amplitude of each frequency component over time.

From Fig. 5, the changing colors indicate that PK method detects the amplitude variation in the frequency of 60 Hz, while the amplitudes of the others remain constant in time.

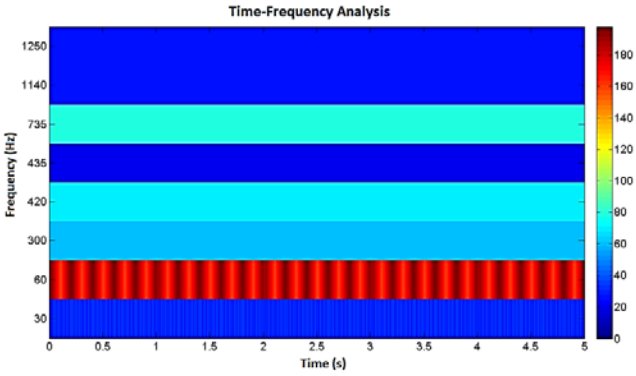

Fig. 5 Time-Frequency Diagram fory(t)obtained by PK

Although y(t) is a synthetic signal, its THD and TID levels are similar to those seen in inverters of some photovoltaic installations. These indicators, with respect to current, undergo significant changes over time, especially when the power delivered to the network is low [13].

Open Science Index, Electrical and Computer Engineering Vol:9, No:11, 2015 publications.waset.org/10003180.pdf

B. Signals of a Photovoltaic Generation Installation

Fig. 6 shows the evolution of the RMS current value measured in a photovoltaic installation between 11h00 and 12h00.

Fig. 7 shows the spectrain the form of time-frequency diagrams obtained with the application of each method during the considered measurement period. The results are shown for the aggregation of 180 cycles.

From Fig. 7 it can be observed through the changing colors that the two methods detect the variation of amplitude in frequency of 60 Hz. Furthermore, the presence of a DC component variant in time and sub-harmonics is noted in Fig. 7. The presence of these components was expected, since the waveform of the signal presents a variable DC level, and a modulation envelope [9]. This behavior was observed throughout the measurement period.

With the application of PK method, it is possible to observe the behavior of the bars which are invisible to DFT (for example, for frequencies of 34 Hz, 43 Hz and 54 Hz). Indeed, PK method allows a more detailed view of the spectrum, because it has a higher spectral resolution. The temporal variations in the PK spectrum are more compatible to those observed in the measurements of current, which, as explained in Fig. 6, showed significant changes in the period from 11h00 to 12h00. It can be justified by the operations of the photovoltaic panels and inverters.

The peaks of the current appear in the PK spectrum as small brown intermittent bands on the horizontal bars representing the amplitudes of the DC component and of the 60 Hz component (Fig. 7). These bars are almost absent in the spectrum of the IEC method.

Fig. 8 illustrates the behavior of the magnitude of the fundamental from the current detected by each method along the day of measurement.

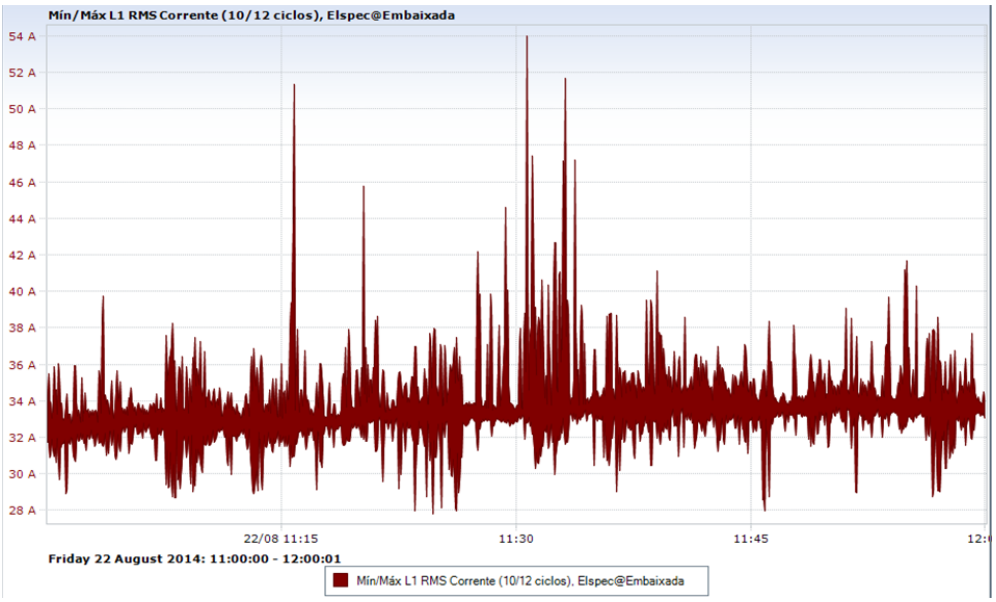

Fig. 6 RMS Current Value Measured in Phase A

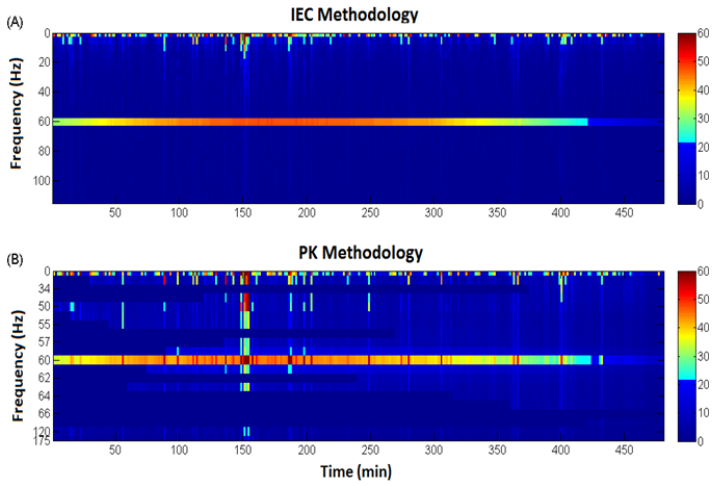

Fig. 7 Time-Frequency Diagram obtained by: (A) Prony-Kalman and (B) IEC. Amplitudes at every 180 cycles

Open Science Index, Electrical and Computer Engineering Vol:9, No:11, 2015 publications.waset.org/10003180.pdf

From Fig. 8, note that the PK method depicts the variations that occur in the evolution of the amplitude of the fundamental, while the IEC method brings the amplitude closer, compensating the real variation with the creation of spurious components in periods in which the fundamental presents highly significant changes (Fig. 7).

Table II shows the P95% values calculated with the application of the IEC and PK methods of the following parameters: THD, TID, RMS of the Fundamental, Individual distortions of harmonics of the 2nd, 3rd and 5th order, and the subgroups of inter-harmonics 0,1 and 2.

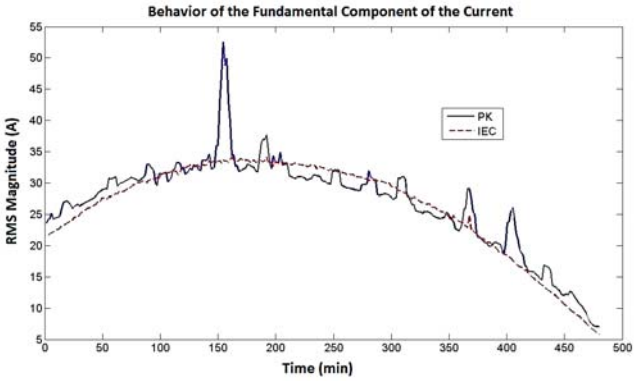

Fig. 8 Evolution of the amplitude of the fundamental in Photovoltaic installation

TABLE II
VALUES OF P95% FOR THE PQ PARAMETERS ACCORDING TO THE IEC AND PK METHODS

Parameters	P95%	
	IEC	PK
THD	31,7%	43,0%
TID	185%	143%
60 Hz	32 A	36 A
2ª	9,7%	14,2%
3ª	11,6%	18,9%
5ª	5,3%	8,6%
Sub. IH 0	172%	124%
Sub. IH 1	13,5%	0%
Sub. IH 2	9,0%	0%

In Table II, it was verified that for the same signal, the methods returned different values. However, it is known according to the results obtained with the synthetic signal analysis that, the information derived from the PK method are more reliable than those from the IEC. For this reason, the P95% obtained from the PK method are, in this study, taken as a reference. It should be mentioned that the high levels of the global distortion of TID registered in the two cases are due to the presence of a DC component with high amplitude.

Fig. 9 shows the evolution of the global distortion indices, TID and THD, returned by each method in the aggregations of 180 cycles over the measurement period. From Fig. 9 the presence of high values of distortion in the current of the installation can be observed. It is noted that the TID levels registered by the IEC method are superior to those registered by the PK method, while the THD levels from IEC are inferior.

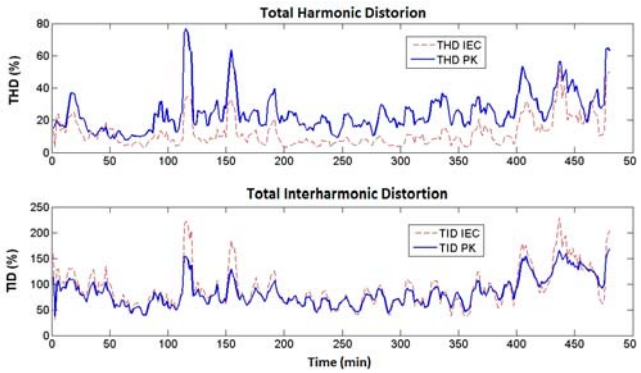

Fig. 9 Evolution of THD and TID in Photovoltaic Installation

V. CONCLUSION

This study was aimed to present the results of a comparative evaluation of a method of measurement based on IEC 61000-4-30 and IEC 61000-4-7 standards and a second from the combination of Prony method with the Kalman filtering. Synthetic signals and data acquired through measurement in a 50 kWp photovoltaic installation were employed for this study.

Based on the results obtained in the simulations with synthetic signals, the comparative analysis of the methods showed that the estimation of the frequencies identified by PK was not significantly affected by temporal variation of the signal, which justifies the exhibition of more reliable results than the IEC method. Also noteworthy is that the Kalman filtering allowed the tracking of variations in the amplitude of the components.

The evaluations conducted with the current of real signals from photovoltaic installation permitted the confirmation of high levels of distortion, and also a time-variant behavior. Based on the results obtained in the evaluations with real signals, despite the two methods detecting the amplitude variation in the 60 Hz frequency, it was found that the PK method permitted a more detailed view of the spectrum, because the spectral resolution was higher. The IEC was unable to detect changes in durations close to or inferior to 12 cycle window. Thus, in the course of the measurement day, it could only follow the slow variations of the RMS value of the fundamental which occurs by a change in the power level generated by the installation.

High levels of global distortion were observed in THD and especially in the TID. The latter is related to the presence of a DC component with quite significant amplitude in the signal. It was observed that the TID levels registered by the IEC method were higher than those registered by the PK method. Conversely, the THD levels from IEC were lower. This is justified by the presence of spurious inter-harmonic components in the spectrum arising from the application of the IEC method, which were not verified in the PK method.

Although the application of the PK method appears to have a more reliable result, it can be emphasized that the processing time is significantly higher than that of the IEC method, which can jeopardize their use for some situation.

Based on the results obtained in this study and considering that the methods based on DFT form the basis of most of the standards that guide the measurement of distortions, an investigation aimed to identify the Fourier window and measurement intervals that could yield results close to those presented by the PK method is recommended.

REFERENCE

[1] Reis, A. (2014) Uma Contribuiçãopara o ControleOperativo de UnidadesEólicas: Modelagem, Regulação de Tensão e Minimização das DistorçõesHarmônicas. (Tese) Doutorado - Universidade Federal de Uberlândia, 2014.

[2] Ribeiro, P.F.; Paulillo, G. Aspectos da Qualidade da EnergiaElétrica no Contexto das RedesInteligentes. RevistaQualidade de Energia, Cap. X, p.40-50, Ed. 93, 2012.

[3] Baghzouz, Y. et al. "Time-varying harmonics: Part I - Characterizing measured data", *IEEE Transactions on Power Delivery*, v. 13, n. 3, p. 938-944, July 1998.

[4] Costa, F. F. (2005) Estimação de Harmônicos e Inter-HarmônicosemSistemasElétricos. (Tese) Doutorado – Centro de Ciências e Tecnologia, Universidade Federal de Campina Grande, 2005.

[5] Leonowicz, Z.; Lobos, T.; Rezmer J. "Advanced Spectrum Estimation Methods for Signal Analysis in Power Electronics", *IEEE Transactions on Industrial Electronics*, v. 50, n. 3, p. 514-519, June 2003.

[6] Sachin K. J.; Singh S.N. "Review Harmonics estimation in emerging power system: Key issues and challenges," *Electric Power Systems Research 81*. p. 1754–1766, June 2011.

[7] IEC 61000-4-7, 2002, Testing and measurement techniques – General guide on harmonics and inter-harmonics measurements and instrumentation, for power supply systems and equipment connected thereto.

[8] IEC 61000-4-30, 2011, Testing and measurement techniques – Power quality measurement methods.

[9] Hanzelka, Z.; Bién, A. Harmonics: 3.1.1 Inter-harmonics. Produced in: AGH University of Science and Technology, July, 2004. In: Leonardo Power Quality Initiative (Org. & Ed.) "Power Quality Application Guide", Available online in (30/03/2014): http://admin.staging.copperalliance.eu/docs /librariesprovider5/power-quality-and-utilisation-guide/311-interharmonics.pdf?sfvrsn=4.

[10] Marple Jr., S. L. Digital Spectral Analysis with Applications. Englewood Cliffs: Prentice- Hall, 1987. ISBN 0-13-214149-3.

[11] Gelb, A. et al. Applied Optimal Estimation. London: M.I.T. Press, 1974.

[12] Kalman, R. "A new approach to linear Filtering and prediction problems," *Trans. of the ASMEJ. Basic Eng*., v. 82, p. 35-45, March 1960.

[13] Block, P. A. B. et al. "Power Quality Analyses of a Large Scale Photovoltaic System," The fifth International Renewable Energy Congress - IREC, Tunisia, March 2014.

Open Science Index, Electrical and Computer Engineering Vol:9, No:11, 2015 publications.waset.org/10003180.pdf